

Coupled Control Lyapunov Functions for Interconnected Systems, with Application to Quadrupedal Locomotion

Wen-Loong Ma¹, Noel Csomay-Shanklin¹, Shishir Kolathaya², Kaveh Akbari Hamed³ and Aaron D. Ames¹

Abstract—This paper addresses the problem of formally guaranteeing the stability of interconnected systems with local controllers with a view toward stabilizing quadrupeds viewed as coupled bipeds. In particular, we present a novel framework that views general rigid-body systems as a collection of lower-dimensional systems that are coupled via reaction forces. Stabilizing the corresponding coupled control system can thus be addressed by stabilizing each subsystem coupled through the passive dynamics. The main results of the paper are stability conditions that guarantee convergence for each control subsystem by formulating coupled control Lyapunov functions (CCLFs) using the notion of input-to-state stability (ISS). This theoretical result is illustrated via a simple cart-pole example, where exponential stability is obtained. Next, building on previous results where an 18-DOF quadrupedal robot is decomposed into two interconnected bipedal systems for efficient periodic gait generation, we design model-free quadratic programs (QPs) using the CCLFs to stabilize the continuous dynamics and thus achieve experimental walking and simulated hopping and running on the Vision 60 quadrupedal robot.

Index Terms—Legged Robots, Optimization and Optimal Control; Motion Control

I. INTRODUCTION

IN the past decade, dynamic locomotion of high-dimensional robotic systems such as 3D humanoids and quadrupedal robots have been a benchmark problem in the fields of control and computation. The high nonlinearity of these systems often makes it intractable to design control laws that encode formal guarantees of stability and robustness while being realizable in practice. To address this theory-reality gap, various methods have built on the idea of model simplification to reduce the complexity of locomotion control. The linear inverted pendulum (LIP) model was popularly used to control bipedal systems [1], [2]. The Zero Momentum Point (ZMP) [3] method gives a robust but restrictive condition to prevent foot-rolling. Further, the whole-body control [4] and centroidal dynamics [5] take account of the dominating effect of center of mass to control bipedal and quadrupedal locomotion [6]. Yet these methods lack guarantees with respect to the full-order dynamics.

Manuscript received: October 15, 2020; Revised January 1, 2021; Accepted February 15, 2021.

This paper was recommended for publication by Editor Abderrahmane Kheddar upon evaluation of the Associate Editor and Reviewers' comments. This work was supported by NSF under grant 1724464. The work of K. Akbari Hamed was supported by the NSF under grants 1923216 and 1924617.

¹The California Institute of Technology, Pasadena, CA, 91106, USA (e-mail: {wma, noelcs, ames}@caltech.edu)

²The Department of Computer Science and Automation, Indian Institute of Science, India (e-mail: shishirk@iisc.ac.in)

³The Department of Mechanical Engineering, Virginia Tech, Blacksburg, VA 24061, USA (e-mail: kavehakbarihamed@vt.edu)

Digital Object Identifier 10.1109/LRA.2021.3065174

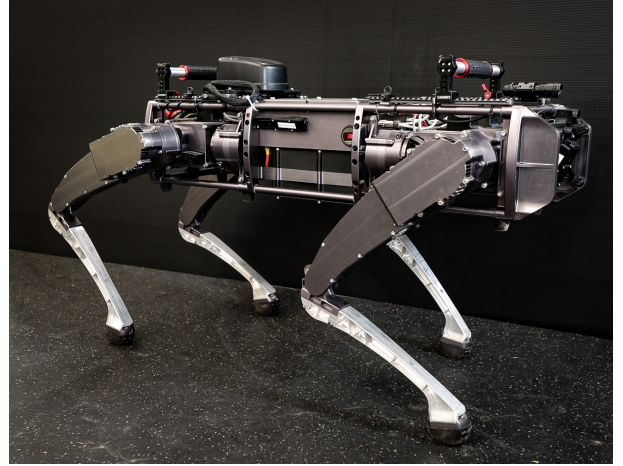


Fig. 1. The quadrupedal robot, Vision 60 v3.9—studied in this work.

From a formal perspective, hybrid zero dynamics (HZDs) [7], [8] reduces the stability of the full-order hybrid dynamics, via control, to the lower-dimensional zero dynamics manifold, thus giving theoretical guarantees that yield experimental success for complex robots [9], [10], [11]. Building on this dimensional reduction concept, the authors previously introduced the framework of coupled control systems (CCSs) [12]. The key idea is that we can view a robotic system as a collection of lower-dimensional nonlinear systems that are coupled via reaction forces enforcing holonomic coupling constraints. By isolating each subsystem from the full-order system, we can leverage this methodology to efficiently optimize quadrupedal gaits. This has been utilized for flat-ground walking and sloped terrain walking [13], [14]. The goal of this paper is to take a first step towards controlling the full-order dynamics of quadrupedal locomotion by stabilizing the continuous dynamics via control Lyapunov functions.

Related Work. The study of coupled dynamical and control systems has a long and rich history from which the method presented in this paper has taken inspiration. First, from the computational perspective, the highly efficient method for calculating the dynamics of robotic systems — spatial vector algebra [15] — uses a similar concept: Lagrange multipliers that enforce holonomic constraints. Second, focusing on the coupled dynamics, the interconnected systems [16] have studied the synchronization of coupled oscillators [17], [18]. Further, the passivity-based control [19] has been proposed to design coupled controllers for multi-agent systems, and the input-to-state stability analysis [20] studied the Lyapunov stability of decoupled control laws. Third, in the control community, the most relevant examples are the multi-agent networks [21], the consensus problem [22] and the cooperative

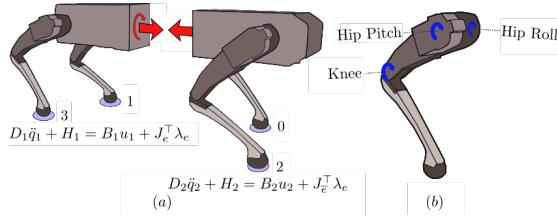


Fig. 2. (a) The decomposition of a quadrupedal robot into two bipedal systems with toe indices labeled and (b) the configuration of the quadruped – each leg has a point contact toe and three rotational joints with motors.

control problem [23], [24]. These methods have been successfully demonstrated on a wide range of robotic applications, especially on drones. However, the problems considered in these frameworks are often coupled on the control level — shared feedback information — but not the dynamics level, such as the general formulation considered in [25]. This allows for the designer to utilize the built-in stabilizing controller of each subsystem to achieve some add-on optimality. In other words, each subsystem’s stability does not critically rely on the other subsystems’. In related work, the coordination of multiple quadrupedal robots via reaction forces has recently been studied [26].

Contribution. Our contributions are twofold. First, through the formulation of coupled control Lyapunov functions, we can formally define the stability criteria of each subsystem while they are dynamically coupled with the rest of the system due to the shared zero dynamics. We can then utilize these Lyapunov functions to synthesize local optimal control laws for each individual subsystem that guarantee stability of the overall coupled control system, and hence the full-order dynamics. Second, when applying to rigid-body dynamics, we can incorporate quadratic programming formulations with two types of Lyapunov functions for controller design. First, feedback linearization based CLFs are synthesized and demonstrated on a cart-pole example showing stability. Second, PD-inspired Lyapunov functions are used to synthesize model-free CLFs for experimental robustness. These CLFs are applied to stabilizing the continuous dynamics of quadrupedal locomotion. This stabilization is demonstrated in simulation with regard to hopping and running. Finally, we demonstrate this framework on hardware, specifically the Vision 60 robot (Fig. 1). We empirically show that it is able to walk stably and robustly on outdoor environments.

Notation. In this paper, we denote the set of non-negative real numbers as \mathbb{R}_+ , the Lie derivative of a function $f(x)$ along the vector field $g(\cdot)$ is defined as $L_{g(\cdot)}f(x) \triangleq \frac{\partial f(x)}{\partial x}g(\cdot)$. The Euclidean norm of a vector of proper dimension is $|\cdot|$, and we take $\|d\|_\infty \triangleq \sup_{t \geq 0} (|d(t)|)$. The matrix norm induced by the Euclidean vector norm is $\|\cdot\|_2$, and the distance from a point (x, z) to a periodic orbit is $\|(x, z)\|_O \triangleq \inf_{(x', z') \in O} |(x, z) - (x', z')|$.

II. BACKGROUND: COUPLED CONTROL SYSTEMS

It was shown in [13] how the dynamics of quadrupedal robots can be decomposed into bipedal robots. As a means of generalizing this methodology, the framework of coupled

control systems was introduced in [12]. Here we review the constructions in these papers to set the stage for the results presented in this paper—synthesizing stabilizing controllers for coupled control systems via control Lyapunov functions. Importantly, we provide a slightly different variation of coupled control systems suited to studying stability.

Given a system composed of multiple interconnected rigid-bodies, the equations of motion (EOMs) of the *full-body dynamics* (also referred as full-order dynamics) can be obtained through Euler–Lagrange equations:

$$D(q)\ddot{q} + H(q, \dot{q}) = B(q)u \quad (1)$$

where $q \in \mathcal{Q} \subset \mathbb{R}^n$ contains the configuration coordinates, $D(q) \in \mathbb{R}^{n \times n}$ is the mass-inertia matrix, $H(q, \dot{q}) \in \mathbb{R}^n$ represents the Coriolis force and gravity, $B(q) \in \mathbb{R}^{n \times m}$ is the actuation matrix which maps the inputs to the configuration space, and $u \in \mathcal{U} \subset \mathbb{R}^m, m \leq n$ is the control input. More details can be found in [15], [27].

In this paper, we are interested in the dynamical systems that can be considered as a collection of two subsystems with index $i \in \{1, 2\} \triangleq \mathcal{N}$. We first define subsystem configurations as $q_i \in \mathcal{Q}_i \subset \mathbb{R}^{n_i}$ such that $\cup_{i \in \mathcal{N}} \iota_i(\mathcal{Q}_i) = \mathcal{Q}$ with $\iota_i : \mathcal{Q}_i \rightarrow \mathbb{R}^n$ as a canonical embedding. Since the goal is to control each subsystem individually, the subsystem inputs are defined as components of the full-system inputs $u^\top = (u_1^\top, u_2^\top)$ with $u_i \in \mathcal{U}_i \in \mathbb{R}^{m_i}$ and $\sum_{i \in \mathcal{N}} m_i = m$. We also define a set of edges $\mathcal{E} \triangleq \{(1, 2), (2, 1)\}$ representing the subsystems’ connection.

For a dynamical system that are composed of two subsystems (coupled via constraints), such as the *coupled mechanical systems* considered in Fig. 2 and [13], [26], we have

$$\begin{cases} D_1\ddot{q}_1 + H_1 = B_1u_1 + J_e^\top \lambda_e \\ D_2\ddot{q}_2 + H_2 = B_2u_2 + J_{\bar{e}}^\top \lambda_{\bar{e}} \\ \text{s.t. } c_{e,q}(q_1, q_2) \equiv 0, \quad \lambda_e + \lambda_{\bar{e}} = 0 \end{cases} \quad (2)$$

where $\lambda_e, \lambda_{\bar{e}} \in \Lambda_i \in \mathbb{R}^{l_i}$ are the coupling forces and $c_{e,q}$ is the coupling constraint. We can solve the connection force explicitly to reach the form in (1) using

$$\begin{aligned} \lambda_e = -\lambda_{\bar{e}} = & (J_e D_1^{-1} J_e - J_{\bar{e}} D_2^{-1} J_{\bar{e}})^{-1} [J_e D_1^{-1} (H_1 - B_1 u_1) \\ & + J_{\bar{e}} D_2^{-1} (H_2 - B_2 u_2) - \dot{J}_e \dot{q}_1 - \dot{J}_{\bar{e}} \dot{q}_2] \end{aligned} \quad (3)$$

where $J_e(q_1, q_2) = \partial c_{e,q} / \partial q_i$ and $e \triangleq (i, j), \bar{e} \triangleq (j, i) \in \mathcal{E}$.

Subsystem dynamics in output coordinates. After defining the subsystem with an index set \mathcal{N} , we can pick the outputs (the features that we are interested in controlling) of each i^{th} subsystem as

$$y_i(q_i) = y_i^a(q_i) - y_i^d(q_i) \quad (4)$$

where $y_i^d, y_i^a \in \mathbb{R}^{m_i}$ are the *desired* outputs and the *actual* outputs, respectively. Since y_i is a function of the “positional states” q_i , it has a relative degree two with respect to the control inputs. We then have the i^{th} subsystem dynamics in output coordinates as

$$\ddot{y}_i = \mathcal{L}_i(q, \dot{q}) + \mathcal{A}_i(q)u_i + \mathcal{A}_{ji}(q)u_j \quad (5)$$

for all $i \in \mathcal{N}$. Note that $\mathcal{A}_{ji}(q) \in \mathbb{R}^{m_i \times m_j}$ maps u_j with $j \neq i$ to the configuration space of the i^{th} subsystem.

Depending on the given EOMs, there are different ways to obtain the expressions efficiently in (5). One direct method from (1) is given as

$$\begin{bmatrix} \mathcal{L}_1(q, \dot{q}) \\ \mathcal{L}_2(q, \dot{q}) \end{bmatrix} = j_y \dot{q}^2 - J_y D^{-1} H \triangleq \mathcal{L}(q, \dot{q})$$

$$\begin{bmatrix} \mathcal{A}_1(q) \\ \mathcal{A}_{12}(q) \end{bmatrix} - \begin{bmatrix} \mathcal{A}_{21}(q) \\ \mathcal{A}_2(q) \end{bmatrix} = J_y D^{-1} B \triangleq \mathcal{A}(q), \quad (6)$$

where $J_y = \partial y / \partial q$ with the full-system outputs are denoted as $y = (y_1^\top, y_2^\top)^\top$.

Coupled Control Systems. For underactuated systems where $m < n$, zero dynamics will show up in the transition to output coordinates (see [28]). It has been shown that there exists a change of coordinates via a diffeomorphism:

$$\begin{bmatrix} q_1 \\ \dot{q}_1 \\ q_2 \\ \dot{q}_2 \end{bmatrix} \mapsto \begin{bmatrix} \eta_1 \\ \eta_2 \\ z \end{bmatrix}$$

which yields a set of dynamic equations representing the *coupled control system*:

$$\mathcal{C}_c \triangleq \begin{cases} \ddot{y}_1 = \mathcal{L}_1(\eta, z) + \mathcal{A}_1(\eta, z)u_1 + \mathcal{A}_{21}(\eta, z)u_2 \\ \ddot{y}_2 = \mathcal{L}_2(\eta, z) + \mathcal{A}_2(\eta, z)u_2 + \mathcal{A}_{12}(\eta, z)u_1 \\ \dot{z} = \omega(\eta, z) \end{cases} \quad (7)$$

where $\eta = (\eta_1^\top, \eta_2^\top)^\top \in \mathcal{X}$ are the “controlled states”, and $\eta_i = (y_i^\top, \dot{y}_i^\top)^\top$. Note that both \mathcal{L} and \mathcal{A} now depend on the new coordinates η, z . The z -dynamics, $\dot{z} = \omega(\eta, z)$, are regarded as the *internal dynamics* with $z \in \mathcal{Z}$, and we call $\dot{z} = \omega(0, z)$ the *zero dynamics*, i.e., the dynamics on the zero dynamics manifold:

$$\mathbf{Z} = \{(\eta, z) \in \mathcal{X} \times \mathcal{Z} : \eta_i = 0, \forall i \in \mathcal{N}\}. \quad (8)$$

We assume $\omega(\eta, z)$ is locally Lipschitz in η . Note that we can also convert the formulation given by [12, Eq.1] into the form of (7) again by using (3). In this form, not only are the dynamics of each subsystem coupled through the shared zero dynamics coordinates, but the inputs are also coupled, i.e. u_j ($i \neq j$) appears in the i^{th} subsystem dynamics.

III. COUPLED CONTROL LYAPUNOV FUNCTIONS

To design local controllers for the i^{th} subsystem that are independent of the “disturbance” caused by the other subsystems’ inputs, we first introduce the *nominal inputs* that are built using the zero dynamics. We then introduce the main result of this paper, a theorem that leads to the synthesis of a networked control architecture. It is this controller that later enables us to control each sub-bipedal system individually with stability guarantees.

A. Disturbed subsystem.

Before designing the control law $u(x) \triangleq \{u_i(x)\}_{i \in \mathcal{N}}$, we first give the concept of a *nominal control input* in the following definition.

Definition 1. The control input that renders the zero dynamics surface $\mathcal{Z} \triangleq \{(q, \dot{q}) : y_i = \dot{y}_i = 0, \forall i \in \mathcal{N}\}$ forward-invariant is the *nominal input* for a coupled control system (7), i.e.,

$$0 = \mathcal{L}_i(0, z) + \mathcal{A}_i(0, z)u_i^Z + \mathcal{A}_{ji}(0, z)u_j^Z \quad (9)$$

for all $i \in \mathcal{N}$. We further define $u^Z(z) \triangleq \{u_i^Z(z)\}_{i \in \mathcal{N}}$.

For the rigid-body dynamics of interest, the decoupling matrix $\mathcal{A}(0, z)$ is assumed to be invertible. Hence, the unique controller that satisfies (9) would be as follows:

$$u^Z(z) = -\mathcal{A}^{-1}(0, z)\mathcal{L}(0, z) \triangleq \begin{bmatrix} u_1^Z \\ u_2^Z \end{bmatrix}. \quad (10)$$

Disturbed subsystem. By considering the nominal control input u_j^Z of the j^{th} subsystem ($j \neq i$), we can reformulate the subsystem dynamics (5) to remove the dependence on the other interconnected (coupled) subsystem’s control input. Concretely, we have

$$\begin{aligned} \ddot{y}_i &= \mathcal{L}_i(\eta, z) + \mathcal{A}_i(\eta, z)u_i + \mathcal{A}_{ji}(\eta, z)(u_j + u_j^Z(z) - u_j^Z(z)) \\ &= \mathcal{L}_i(\eta, z) + \mathcal{A}_{ji}(\eta, z)u_j^Z(z) + \mathcal{A}_i(\eta, z)u_i \\ &\quad + \underbrace{\mathcal{A}_{ji}(\eta, z)(u_j - u_j^Z(z))}_{\triangleq d_e} \end{aligned} \quad (11)$$

where we denote

$$d_e(\eta, z, u_j) \triangleq \mathcal{A}_{ji}(\eta, z)(u_j - u_j^Z(z)), \quad e \triangleq (j, i) \quad (12)$$

as the *disturbance* induced by the j^{th} subsystem’s inputs to the i^{th} subsystem. Having established the disturbed subsystem dynamics as in (11), the coupled control system in (7) becomes a *disturbed coupled control system*, as:

$$\mathcal{C}_c^d \triangleq \begin{cases} \ddot{y}_1 = \mathcal{L}_1(\eta, z) + \mathcal{A}_{21}(\eta, z)u_2^Z(z) + \mathcal{A}_1(\eta, z)u_1 + d_e \\ \ddot{y}_2 = \mathcal{L}_2(\eta, z) + \mathcal{A}_{12}(\eta, z)u_1^Z(z) + \mathcal{A}_2(\eta, z)u_2 + d_e \\ \dot{z} = \omega(\eta, z) \end{cases} \quad (13)$$

where each subsystem is only subject to local controller and a disturbance term. This is where we can utilize input-to-state stabilizing control Lyapunov functions to reject the disturbance while stabilizing each subsystem.

Remark 1. Note that the overall disturbance vanishes on the invariant zero dynamics manifold \mathbf{Z} , i.e., $d(0, z, u_i^Z) = \{d_e(0, z, u_i^Z)\}_{\forall e \in \mathcal{E}} = 0$. This can be seen by plugging $u_i(0, z) = u_i^Z$ from (9) into (11), whereby

$$0 = \mathcal{L}_i(0, z) + \mathcal{A}_{ji}(0, z)u_j^Z + \mathcal{A}_i(0, z)u_i^Z + d_e = 0 + d_e,$$

which yields $d_e = 0$ and further $d = 0$.

B. CLF from the viewpoint of ISS.

In order to guarantee stability, from which we eventually synthesize the local control laws, we first present the following definitions that are the foundation of this paper. With some modifications of [29] to fit the context of this paper, we have the following.

Definition 2. A smooth function $V_i : \mathbb{R}^{n_i} \rightarrow \mathbb{R}_+$ is an *input-to-state stabilizing control Lyapunov function (ISS-CLF)* for $\dot{\eta}_i = f(\eta, z) + g(\eta, z)(u_i + d_e)$ with $\eta_i \in \mathbb{R}^{n_i}$, if there exists constants $c_1, c_2, c_3 > 0$, $\varepsilon \in (0, 1)$, $\bar{\varepsilon} > 0$ such that $\forall \eta, z, d$,

$$c_1 |\eta_i|^2 \leq V_i(\eta_i) \leq \frac{c_2}{\varepsilon^2} |\eta_i|^2 \quad (14)$$

$$\inf_{u_i \in \mathcal{U}_i} \left(L_f V_i(\eta, z) + L_g V_i(\eta, z)u_i + \frac{c_3}{\varepsilon} V_i(\eta_i) + \frac{1}{\bar{\varepsilon}} |L_g V_i|^2 \right) \leq 0.$$

The construction of Def. 2 is motivated by the *rapidly exponentially stabilizing control Lyapunov function (RES-CLF)* from [8]. Based on Def. 2, we can form a class of control laws directly:

$$K_i(\eta, z) \triangleq \left\{ u_i \in \mathcal{U}_i : L_{f_i} V_i + L_{g_i} V_i u_i + \frac{c_{3,i}}{\varepsilon_i} V_i + \frac{1}{\varepsilon_i} |L_{g_i} V_i|^2 \leq 0 \right\}, \quad (15)$$

which yields the set of control values which satisfy the desired convergence property for each subsystem $i \in \mathcal{N}$. The (constant) parameters $c_{1,i}, c_{2,i}, c_{3,i}, \varepsilon_i, \bar{\varepsilon}_i$ are associated with each subsystem with $i \in \mathcal{N}$.

We now present the main theorem of this paper that guarantees the stability of the disturbed coupled control system by taking values from $K_i(\eta, z)$, $\forall i \in \mathcal{N}$.

Theorem 1. *For a dynamical system given by*

$$\mathcal{C}^z \triangleq \begin{cases} \dot{\eta}_1 = f_1(\eta, z) + g_1(\eta, z)(u_1 + d_e) \\ \dot{\eta}_2 = f_2(\eta, z) + g_2(\eta, z)(u_2 + d_e) \\ \dot{z} = \omega(\eta, z) \end{cases}, \quad (16)$$

let \mathcal{O}_z be an exponentially stable periodic orbit of the zero dynamics $\dot{z} = \omega(0, z)$. If there exists an ISS-CLF $V_i(\eta_i)$ for each subsystem $i \in \mathcal{N}$, then for all locally Lipschitz continuous feedbacks $u_i(x) \in K_i(x)$ given by (15), the full-order periodic orbit $\mathcal{O} \triangleq \iota(\mathcal{O}_z)$ is ultimately bounded, with the bounds tending to zero as $|d_e|, |d_{\bar{e}}| \rightarrow 0$.

Proof. First, we use the converse Lyapunov theorem from [30] to construct the following Lyapunov function for the zero dynamics. Given \mathcal{O}_z is an exponentially stable periodic orbit of \mathcal{Z} , there exists a Lyapunov function $V_z : \mathcal{Z} \rightarrow \mathbb{R}_+$ such that in a neighbourhood $B_\delta(\mathcal{O}_z)$ of \mathcal{O}_z ,

$$r_1 \|z\|_{\mathcal{O}_z}^2 \leq V_z(z) \leq r_2 \|z\|_{\mathcal{O}_z}^2, \\ \dot{V}_z(z) \leq -r_3 \|z\|_{\mathcal{O}_z}^2, \quad \left| \frac{\partial V_z}{\partial z} \right| \leq r_4 \|z\|_{\mathcal{O}_z}.$$

Next we have the following Lyapunov function candidate for the full-order system:

$$V(\eta, z) = \sum_i V_i(\eta_i) + \sigma V_z(z)$$

It is clear that $V(\eta, z)$ satisfies the first inequality in Def. 2¹. We first take the derivative of the subsystems' Lyapunov functions to get:

$$\begin{aligned} \sum_i \dot{V}_i &= \sum_i L_{f_i} V_i + L_{g_i} V_i u_i + L_{g_i} V_i d_i \\ &\leq \sum_i -\frac{c_{3,i}}{\varepsilon_i} V_i - \frac{1}{\varepsilon_i} |L_{g_i} V_i|^2 + |L_{g_i} V_i| |d_i| \\ &\leq \sum_i -\frac{c_{3,i}}{\varepsilon_i} V_i - \left(\frac{1}{\sqrt{\varepsilon_i}} |L_{g_i} V_i| - \sqrt{\varepsilon_i} \frac{\|d\|_\infty}{2} \right)^2 + \varepsilon_i \frac{\|d\|_\infty^2}{4} \\ &\leq \sum_i -\frac{c_{3,i}}{\varepsilon_i} V_i(\eta_i) + \varepsilon_i \frac{\|d\|_\infty^2}{4} \\ &\leq -\min_i \left(\frac{c_{3,i}}{\varepsilon_i} c_{1,i} \right) |\eta|^2 + \frac{\max_i(\bar{\varepsilon}_i)}{2} \|d\|_\infty^2, \end{aligned}$$

Then the total derivative of the Lyapunov function becomes:

¹The definition of Lyapunov functions for an invariant set, such as periodic orbits, can be found in [31].

$$\begin{aligned} \dot{V} &= \sigma \frac{\partial V_z}{\partial z} w(0, z) + \sigma \frac{\partial V_z}{\partial z} (w(\eta, z) - w(0, z)) + \sum_i \dot{V}_i \\ &\leq -\sigma r_3 \|z\|_{\mathcal{O}_z}^2 + \sigma r_4 \|z\|_{\mathcal{O}_z} |w(\eta, z) - w(0, z)| + \sum_i \dot{V}_i \\ &\leq -\sigma r_3 \|z\|_{\mathcal{O}_z}^2 + \sigma r_4 \|z\|_{\mathcal{O}_z} L_z |\eta| + \sum_i \dot{V}_i \\ &\leq -\sigma r_3 \|z\|_{\mathcal{O}_z}^2 + \sigma r_4 L_z \|z\|_{\mathcal{O}_z} |\eta| - \underbrace{\min_i \left(\frac{c_{3,i}}{\varepsilon_i} c_{1,i} \right)}_{r_6} |\eta|^2 \\ &\quad + \frac{\max_i(\bar{\varepsilon}_i)}{2} \|d\|_\infty^2, \\ &= -[\|z\|_{\mathcal{O}_z} \quad |\eta|] \Lambda \begin{bmatrix} \|z\|_{\mathcal{O}_z} \\ |\eta| \end{bmatrix} + \frac{\max_i(\bar{\varepsilon}_i)}{2} \|d\|_\infty^2, \end{aligned}$$

with L_z the Lipschitz constant for $\omega(\eta, z)$ and

$$\Lambda = \begin{bmatrix} \sigma r_3 & -\frac{1}{2} \sigma r_4 L_z \\ -\frac{1}{2} \sigma r_4 L_z & r_6 \end{bmatrix}$$

we then can pick σ such that Λ is positive definite, i.e., V is a Lyapunov function for the periodic orbit $\mathcal{O} = \iota(\mathcal{O}_z)$. \square

The proof is inspired by the construction of [8, Appx.B]. We note that an effective way to reduce the effect of the disturbance is to decrease $\bar{\varepsilon}_i$. Further, since ISS-CLF is one robust type of CLFs, we will continue to use the terminology CLFs for clarity². Since these CLFs are defined around the coupled control systems, we call $\{V_1, V_2\}$ the **coupled control Lyapunov functions (CCLFs)**. Further, we can obtain exponential stability for the full-order system under certain conditions, which are summarized as follows.

Corollary 1. *In addition to the prerequisites given by Thm.1, if we additionally have*

$$|d(t)| \leq c_4 |\eta(t)| \text{ and } \left| \sum_i L_{g_i} V_i \right| \leq c_5 |\eta| \quad \forall \eta, \quad (17)$$

the solution to the full-order dynamics in (16) is exponentially stable provided that $2 \min_i \left(\frac{c_{3,i}}{\varepsilon_i} \right) > c_4 c_5 \min_i (c_{1,i})$.

Proof sketch. Due to space limitation, we omitted the detailed proof. But the basic idea is that given these conditions, we can establish $|\sum_i L_{g_i} V_i| |d| \leq c_4 c_5 |\eta|^2$ for the full-order system, and the disturbance d vanishes as the controlled states $\{\eta_i\}_{i \in \mathcal{N}}$ converge to the zero dynamics surface. \square

Note that for a general situation when the disturbance does not completely vanish on the zero dynamics surface, i.e., $|d(t)| \leq c_4 |\eta| + c_6 |z| + c_7$, the system exponentially converges to a ultimate bound for robotic dynamics. Due to space limitation, this will be addressed in future work.

Stability constraint. As the theorem suggested, we can thus construct the local control Lyapunov functions for a coupled control system. Following the construction of (15), we have a class of controllers using a linear constraint of the input:

$$\rho_i(\eta, z) + \psi_i(\eta, z) u_i + \frac{1}{\varepsilon_i} |\psi_i(\eta, z)|^2 \leq 0 \quad (18)$$

²Note that for the class of robotic systems of interest (such as the quadruped in Fig. 2), it can be shown that any CLF qualifies as an ISS-CLF (see [32]). In other words, the set given by (15) needs not have $L_{g_i} V_i$.

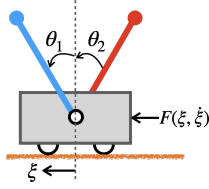


Fig. 3. A cart-pole system with two inverted pendula, each is directly actuated by a motor. The mass of the cart and a pendulum are $2M$ and m , correspondingly. The length of both pendulum is l .

where $\rho_i(\eta, z) = L_{f_i} V_i(\eta, z) + \frac{\gamma}{\varepsilon_i} V_i(\eta_i)$ and $\psi_i(\eta, z) = L_{g_i} V_i$. A practical control law that satisfies (18) is a minimum-norm in $K_i(\eta, z)$, given by

$$m_i(\eta, z) = \operatorname{argmin}\{ |u_i|^2 : u_i \in K_i(\eta, z) \}, \quad (19)$$

which can then be solved by some quadratic programming (QP) algorithm.

C. Control synthesis for cart-pole

We now show an example for applying the coupled control Lyapunov functions to a 3-DOF mechanical system. For the modified cart-pole system shown in Fig. 3, ξ is the horizontal displacement of the cart, and θ_1, θ_2 are the angles of the two joints, each of which is actuated by a motors. We denote the inputs as u_1, u_2 . The full system is also subject to a force function given by $F(\xi, \dot{\xi}) = 2(m + M)(-\xi + \dot{\xi}(1 - \xi^2 - \dot{\xi}^2))$. Separated by the dashed line as Fig. 3, we can view each pendulum-cart system as a subsystem with index $i \in \mathcal{N} \triangleq \{1, 2\}$. Let the subsystem configuration be $q_i = (\xi, \theta_i)$. With a target to control the outputs (a.k.a. the virtual constraint [7]), we define the subsystem output as $y_i(q_i) = \theta_i$ for the i^{th} subsystem with $i \in \mathcal{N}$. In other words, the goal is to drive both pendula upright as $t \rightarrow \infty$ using local controllers. With the output Jacobian obtained by

$$y(q) = \begin{bmatrix} y_1(q_1) \\ y_2(q_2) \end{bmatrix} \Rightarrow J_y \triangleq \frac{\partial y}{\partial q} = \begin{bmatrix} 0 & 1 & 0 \\ 0 & 0 & 1 \end{bmatrix},$$

we can use (6) to obtain the dynamics in the form of coupled control systems, as in (7). Note that the zero dynamics $\dot{z} = \omega(\mathbf{0}, z)$ — when $\theta_i = \dot{\theta}_i = 0, \forall i \in \mathcal{N}$ — become a Van der Pol oscillator due to the force function: $\ddot{\xi} = F(\xi, \dot{\xi})/(2m + 2M)$. This system is known to have a globally exponentially stable periodic solution, denoted by \mathcal{O}_z .

For rigid-body dynamics with invertible decoupling matrices \mathcal{A}_\square , we can apply an input-output feedback-linearization:

$$u_i(\eta, z) = \mathcal{A}_i^{-1}(\eta, z) \left(-\mathcal{L}_i(\eta, z) - \mathcal{A}_{j_i}(\eta, z) u_j^Z(z) + \mu_i \right) \quad (20)$$

with μ_i the *auxiliary input* for each subsystem $i \in \mathcal{N}$. The nominal control input u_j^Z with $j \neq i$ is then given by (10). The subsystem output dynamics now become:

$$\ddot{y}_i = \mu_i + d_e. \quad (21)$$

If we define $\eta_i = (y_i^\top, \dot{y}_i^\top)^\top$, we can obtain the linearized subsystem dynamics as

$$\dot{\eta}_i = \underbrace{\begin{bmatrix} 0 & I \\ 0 & 0 \end{bmatrix}}_F \eta_i + \underbrace{\begin{bmatrix} 0 \\ I \end{bmatrix}}_G (\mu_i + d_e), \quad (22)$$

which is in the form of (16). Therefore, we can define the coupled control Lyapunov functions according to Thm.1. Concretely, for each subsystem i , we have

$$V_i(\eta_i) = \eta_i^\top P_i \eta_i, \text{ with } P_i \triangleq \begin{bmatrix} \frac{1}{\varepsilon_i} I & 0 \\ 0 & I \end{bmatrix} P \begin{bmatrix} \frac{1}{\varepsilon_i} I & 0 \\ 0 & I \end{bmatrix}. \quad (23)$$

with $\varepsilon_i \in (0, 1)$ a constant and $P \in \mathbb{R}^{2 \times 2}$ the solution to the *continuous time algebraic Riccati equation* (CARE). More details can be found in [8, Sec.3].

Remark 2. Based on the CCLFs chosen, an appropriate control can be constructed that yields control robustness. For example, using the feedback linearization of the form (20) we can choose the control law as:

$$u_i = \mathcal{A}_i^{-1} \left(-\mathcal{L}_i - \mathcal{A}_{j_i} u_j^Z - \frac{1}{\varepsilon_i^2} K_p y_i - \frac{1}{\varepsilon_i} K_d \dot{y}_i - \frac{1}{\varepsilon_i} L_G V_i^\top \right) \quad (24)$$

where $K_p, K_d \succeq 0$. This controller, inspired by [33], is a specific example that belongs to the set $K_i(\eta, z)$.

CLF-QP. We now present the QP formulation that calculates control values using the chosen CLFs. Note that μ_i is only an auxiliary input instead of the actual system-level input. We will replace it with u_i for better numerical conditioning for the optimal control problem. Based on (20) we have μ_i as a function of u_i :

$$\mu_i = \mathcal{L}_i + \mathcal{A}_{j_i} u_j^Z + \mathcal{A}_i u_i$$

then the stability condition (18) can be re-written as:

$$\rho_i + \psi_i(\mathcal{A}_i u_i + \mathcal{L}_i + \mathcal{A}_{j_i} u_j^Z) + \frac{1}{\varepsilon_i} |\psi_i|^2 \leq 0, \quad (25)$$

$$\begin{aligned} \text{with } \rho_i &= L_F V_i + \frac{\gamma}{\varepsilon_i} V_i = \eta_i^\top (F^\top P_i + P_i F) \eta_i + \frac{\gamma}{\varepsilon_i} V_i, \\ \psi_i &= L_G V_i = 2\eta_i^\top P_i G. \end{aligned}$$

Finally, we have the following QP formulation that encodes the CLF for subsystem $i \in \mathcal{N}$:

$$\begin{aligned} u_i^* &= \operatorname{argmin}_{u_i \in \mathcal{U}_i} \left| \mathcal{L}_i + \mathcal{A}_{j_i} u_j^Z + \mathcal{A}_i u_i \right|^2 \\ \text{s.t. } (C1) \quad &\rho_i + \psi_i(\mathcal{A}_i u_i + \mathcal{L}_i + \mathcal{A}_{j_i} u_j^Z) + \frac{1}{\varepsilon_i} |\psi_i|^2 \leq 0 \\ (C2) \quad &-u_{\max} \preceq u_i \preceq u_{\max} \end{aligned} \quad (26)$$

where, (C1) is the stability constraint, and (C2) is added according to the actual torque bounds from the physical actuators to guarantee the realizability. We regarded (26) the *CLF-QP for coupled mechanical systems*.

Remark 3. With both subsystem taking values from $K_i(\eta, z)$, we have the disturbance as

$$d_e(\eta, z) = \mathcal{A}_{j_i}(\eta, z)(u_j(\eta, z) - u_j^Z(z)).$$

Assuming $d(\eta, z)$ to be locally Lipschitz in η yields

$$|d(\eta, z) - d(\mathbf{0}, z)| \leq c_4 \|\eta - \mathbf{0}\| \Rightarrow |d| \leq c_4 \|\eta\|$$

with c_4 the Lipschitz constant. An effective way to reduce c_4 is to form an optimization problem inside a tube around the given desired trajectory \mathcal{O} , i.e. $\min_{\max} _{(\eta, z) \in \text{tube near } \mathcal{O}} |d(\eta, z)| / \|\eta\|$. Additionally, we have

$$\left| \sum L_G V_i \right| = \left| 2 \sum \eta_i^\top P_i G \right| \leq 2 \|\eta\| \sum \|P_i G\|_2.$$

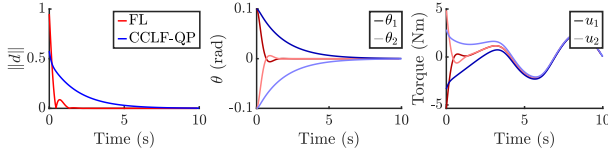


Fig. 4. The cart-pole simulation. Data labeled FL (red) used the feedback linearization controller (24); Data labeled CCLF-QP (blue) used the controller (26). Dark and light variants of the colors are used to distinguish between the first and second pendula. Both simulations show stability.

Hence, if we pick $c_5 = 2 \sum \|P_i G\|_2$, we can obtain exponential stability for the periodic solution to the full-order system according to Corollary 1.

Simulation. We present two simulation results (see Fig. 4 and video [34]) to demonstrate this stability result. As shown in Fig. 3, we pick the model as $l = 0.5, M = 15, m = 5$. Given an initial condition $x(0) = (0, 0.1, -0.1, 0.1, 0, 0)^T$, we first simulate the specific control law given by (24) with $K_p = 5, K_d = 0.1, \varepsilon_i = 0.5, \bar{\varepsilon}_i = 0.5$. Then we simulate the decentralized optimal controller given by (26) with $\varepsilon_i = 0.5, \bar{\varepsilon}_i = 0.5$. The data is shown in Fig. 4. As Corollary 1 suggests, both simulations show exponential stability, and the disturbance vanishes on the zero dynamics surface.

IV. QUADRUPEDAL WALKING WITH MODEL-FREE CLFs

We can also use local CLFs to stabilize the overall system for more complicated robots, such as quadrupedal locomotion. In this section, we will apply the local control laws to an 18-DOF quadrupedal robot (see Fig. 1) by viewing it as two connected bipedal robots. The advantage is that we simultaneously consider each subsystem's stability through the local CLFs, as well as the feasibility conditions such as the motor torque saturation.

For the robot shown in Fig. 2, we use the floating-base convention [7] to get the full-system configuration $q^T = (\xi^T, \theta_0^T, \theta_1^T, \theta_2^T, \theta_3^T)$, with $\xi \in \mathbb{R}^3 \times \text{SO}(3)$ the body-fixed coordinates of the floating base (the torso), and $\theta_k \in \mathbb{R}^3$ the three joint angles of the k^{th} leg, $k \in \{0, 1, 2, 3\}$. All of the joints are directly driven by electric motors, denoted by $u \in \mathcal{U} \subset \mathbb{R}^{12}$. We then have the (continuous-time) full-order, constrained dynamics for quadrupedal walking as

$$\begin{cases} D\ddot{q} + \tilde{H} = \tilde{B}u + J_s^T F_s \\ J_s \ddot{q} + \dot{J}_s \dot{q} = 0 \end{cases}, \quad (27)$$

where the second equation is obtained by taking the second derivative of the ground contact constraint, which is modeled as holonomic constraints of the stance leg's toe. The Jacobian is $J_s(q) = \partial h_s(q) / \partial q$ with $h_s(q) \in \mathbb{R}^3$ the Cartesian position of the toe. Then, (27) can be converted into the general rigid-body dynamics form $D\ddot{q} + H = Bu$ with

$$\begin{aligned} H(q, \dot{q}) &= \tilde{H} - J_s^T (J_s D^{-1} J_s^T)^{-1} (J_s D^{-1} \tilde{H} - \dot{J}_s \dot{q}) \\ B(q) &= \tilde{B} [I - J_s^T (J_s D^{-1} J_s^T)^{-1} J_s D^{-1}]. \end{aligned}$$

Note that for the gaits of interest, *walking*, *running*, and *hopping*, we have a diagonal double-support phase, and a flight phase. In the flight phase, where none of the toes touch ground, the holonomic constraints are not required. The detailed model of multi-domain behaviors for quadrupedal robots can be

found in [11], and we will not introduce the domain index for the ease of notations. Note that in the hybrid system setting, it was previously shown that RES-CLFs provably stabilize the continuous dynamics in such a way that the hybrid dynamics are also stabilized under the assumption of HZD [8, Thm.2]. This result has been extended to the ISS-CLFs in [29], [35]. Formally encoding this in the CCS formulation for hybrid quadrupedal locomotion will be addressed in future work.

Subsystem outputs and CCS. Similar to [13], we consider a quadrupedal robot as two connected bipedal subsystems — the front biped and rear biped — that are coupled by a connection constraint. We define the set of subsystem indices as $\mathcal{N} = \{f, r\}$, where *f, r* label the *front* and *rear* bipedal systems, correspondingly, and $\mathcal{E} = \{e = (f, r), \bar{e} = (r, f)\}$ represents their connection relations. We then pick the coordinates for these two subsystems as $q_i = (\xi^T, \theta_{i, \text{st}}^T, \theta_{i, \text{nst}}^T)^T \in \mathcal{Q}_i$, where the subscript _{st} marks the joints of the leg that are in contact with the ground, and _{nst} for the swing legs. We then define outputs for each subsystem, the bipeds, as

$$y_i(t, q_i) = y_i^a(t) - y_i^d(q_i) \quad i \in \mathcal{N} \quad (28)$$

where the desired outputs (trajectory) $y_i^d(t) \in \mathbb{R}^6$ is given by a set of Bézier polynomials generated by the CCS optimization in [12]. The actual outputs are picked as

$$y_i^a(q_i) = Y_i q_i = \begin{bmatrix} \theta_{\text{st}, \text{hr}} \\ \theta_{\text{st}, \text{hp}} - \frac{\theta_{\text{st}, \text{k}}}{2} \\ \theta_{\text{st}, \text{k}} \\ \theta_{\text{nst}, \text{hr}} \\ \theta_{\text{nst}, \text{hp}} - \frac{\theta_{\text{nst}, \text{k}}}{2} \\ \theta_{\text{nst}, \text{k}} \end{bmatrix}. \quad (29)$$

where the subscript *hr, hp, k* are short for the *hip-roll*, *hip-pitch*, and *knee* joints. This output structure represents the roll angle, pitch angle and leg length of the *virtual leg*, which is the virtual linkage connecting the hip and the toe. Note that if the quadrupedal robot has nonidentical legs for the front and rear subsystems, we will have a different output structure, i.e., $Y_f \neq Y_r$. This will be an interesting future direction for understanding how to cooperate asymmetric quadrupeds. Next, given the full-system output Jacobian $J_y = \partial y / \partial q$, we can use (6) to obtain the CCS dynamics as in (5).

On the zero dynamics surface where both subsystems' output coordinates remain zero, we have the configuration coordinates and their velocity terms satisfying:

$$(q^Z, \dot{q}^Z) = \{(q, \dot{q}) \mid y_i(q) = \dot{y}_i(q, \dot{q}) = 0, \quad \forall i \in \mathcal{N}\}.$$

The nominal inputs that satisfy the invariant condition (9) can therefore be obtained by

$$u^Z(q^Z, \dot{q}^Z, t) = -A(q^Z)^{-1} \mathcal{L}(q^Z, \dot{q}^Z) \triangleq \begin{bmatrix} u_1^Z \\ u_2^Z \end{bmatrix}. \quad (30)$$

We then can have the disturbed subsystem dynamics as given in (13), after which we can control each bipedal system using the coupled control Lyapunov functions.

Model-free CLF-QP. As mentioned in Section III-B, for the quadruped chosen in this study, any CLF qualifies as an ISS-CLF [32]. Hence, we can choose a specific form of the CLF, which is motivated by the Proportional-Derivative control law-inspired Lyapunov function [36, eq(24)], and use it for the

underactuated bipedal systems. The advantage with this class of CLFs is that the corresponding *stability constraint* can be expressed in a model-free fashion. Therefore, an improved experimental robustness against model uncertainty can be obtained. Formally, we have the following model-free stability constraint:

$$(\alpha_i(y_i)y_i^\top + \dot{y}_i^\top)(K_p y_i + K_d \dot{y}_i) + (\alpha_i(y_i)y_i^\top + \dot{y}_i^\top)J_{y_i^\Lambda}^{-\top} u_i \leq 0 \quad (31)$$

for subsystem $i \in \mathcal{N}$, where, $\alpha_i(y_i) = \frac{k_0}{1+|y_i|}$ with a constant $k_0 > 0$. Concretely, in comparison with (15), $(\alpha_i(y_i)y_i^\top + \dot{y}_i^\top)J_{y_i^\Lambda}^{-1}$ is in the place of $L_{g_i}V_i$ terms, and the remaining terms are in place of $L_{f_i}V_i$ terms. $K_p, K_d \succeq 0$ are the diagonal matrices that form the PD gains. The Jacobian matrix of the actual output with respect to the actuated joints for the i^{th} subsystem is given by $J_{y_i^\Lambda} = \partial y_i / \partial q_i^\Lambda$, where q_i^Λ are the actuated joints of the i^{th} bipedal system. We then have the QP formulation utilizing the model-free CLFs as:

$$\begin{aligned} \underset{u_i \in \mathbb{R}^6, \delta \in \mathbb{R}}{\operatorname{argmin}} \quad & |u_i - u_i^{\text{ref}}|^2 + 1000\delta^2 \\ \text{s.t.} \quad & (\alpha_i(y_i)y_i^\top + \dot{y}_i^\top) \left[(K_p y_i + K_d \dot{y}_i) + J_{y_i^\Lambda}^{-\top} u_i \right] \leq \delta \\ & -u_{\max} \preceq u_i \preceq u_{\max} \end{aligned} \quad (32)$$

for the i^{th} subsystem, where $\delta \geq 0$ is a relaxation for better numerical stability given a high penalty weight of 1000. To formulate a model-free QP problem, we also modify the nominal inputs u_i^Z to a output-feedback PD control law, $u_i^{\text{ref}} = -J_{y_i^\Lambda}^\top (K_p y_i + K_d \dot{y}_i)$.

Simulation. Before enabling the proposed method on hardware, we first validated the CCLF-QP in simulation using a physics engine — RaiSim [37]. In particular, we wish to control this quadrupedal robot as two connected bipedal robots performing quadrupedal behaviors such as walking, hopping and running. All of these behaviors can be generated as a single-domain or multi-domain periodic solutions to the coupled control system using the optimization method introduced in [12]. The specific controller we put to the test to achieve stable tracking of the giving periodic gaits is given in (32). The PD gains $K_p, K_d \succeq 0$ are diagonal matrices, and are picked as the same value across all three simulation tests. As a result, the local controller utilizing CCLFs renders stabilization of the given periodic gaits for walking, hopping and running on Vision 60 in RaiSim. An animation is provided in [34]. We show the gait tiles in Fig. 5, and the phase portraits of the simulation data in Fig. 6.

V. EXPERIMENTAL REALIZATION

Hardware. The robot we studied in this paper is the Vision 60 v3.9 quadrupedal robot from Ghost Robotics. As show in Fig. 1, this robot is 44 kg, 54 cm wide and 50~60 cm tall. It uses a hierarchical computation structure to perform various tasks. In our experiments, we implement the optimal controller with a QP solver *OSQP* on the on-board Jetson AGX Xavier computer from NVIDIA. Furthermore, a 1kHz hard real-time operating system enforces the communication between the mainboard and motor drivers to realize the torque commands from the control algorithm (32).

Experiments and Data Analysis. As a first step towards controlling complex quadrupedal robots to achieve various dynamical behaviors using the local control laws, we conducted some walking experiments on the Vision 60 robot. To avoid robustness challenges caused by model uncertainties, especially unpredictable uncertainties introduced by the terrain dynamics, we applied the model-free QPs in (32). As the supplementary video [34] shows, we are able to achieve robust walking with the Vision 60 on outdoor rough terrains with moderate slope variation and surface roots. We show the gait tiles of the walking experiments in Fig. 5. We also provide a comparison between experimental data, simulation data, and the desired trajectory in Fig. 6. We note that the tracking is ultimately bounded by a tube around the desired trajectory in the continuous domains, which provides empirical evidence for future works formally establishing hybrid stability.

VI. CONCLUSION

In this paper, we presented a framework to design local controllers for interconnected dynamical systems. We first introduced the concept of coupled control systems, which were obtained by viewing the general rigid-body dynamics as a collection of lower-dimensional systems. Building on this idea and using the notion of input-to-state stability, a collection of control Lyapunov functions for each subsystem were shown to be able to yield ultimate boundedness for the solution to the closed-loop system. Based on these coupled control Lyapunov functions, we then synthesized local controllers to stabilize the lower-dimensional subsystems with the confidence of stabilization of the full-order system. Putting this idea into practice, we concluded the paper by designing local controllers for each bipedal subsystem of a quadrupedal robot. The end result was the Vision 60 quadrupedal robot robustly traversing outdoor rough terrains. Future work includes utilizing CCLFs to formally establish the stability of full-order hybrid system models of highly-dynamic quadrupedal locomotion, incorporating reduced-order models to enable planning, e.g., via MPC using LIP models, and extending the framework of coupled control systems to multi-robot collaboration.

REFERENCES

- [1] M. Raibert and E. R. Tello, “Legged robots that balance,” *IEEE Expert*, vol. 1, no. 4, pp. 89–89, Nov 1986.
- [2] S. Kajita, K. Tani, and A. Kobayashi, “Dynamic walk control of a biped robot along the potential energy conserving orbit,” in *IEEE International Workshop on Intelligent Robots and Systems, Towards a New Frontier of Applications*, July 1990, pp. 789–794 vol.2.
- [3] K. Hirai, M. Hirose, Y. Haikawa, and T. Takenaka, “The development of Honda humanoid robot,” in *Robotics and Automation. Proceedings IEEE International Conference on*, May 1998, pp. 1321–1326 vol.2.
- [4] S. Fahmi, C. Mastalli, M. Focchi, and C. Semini, “Passive whole-body control for quadruped robots: Experimental validation over challenging terrain,” *IEEE Robotics and Automation Letters*, vol. 4, no. 3, pp. 2553–2560, 2019.
- [5] D. E. Orin, A. Goswami, and S.-H. Lee, *Centroidal dynamics of a humanoid robot*. Springer, 2013, vol. 35.
- [6] J. Di Carlo, P. M. Wensing, B. Katz, G. Bledt, and S. Kim, “Dynamic locomotion in the MIT Cheetah 3 through convex model-predictive control,” in *2018 IEEE/RSJ International Conference on Intelligent Robots and Systems (IROS)*, Oct 2018, pp. 1–9.

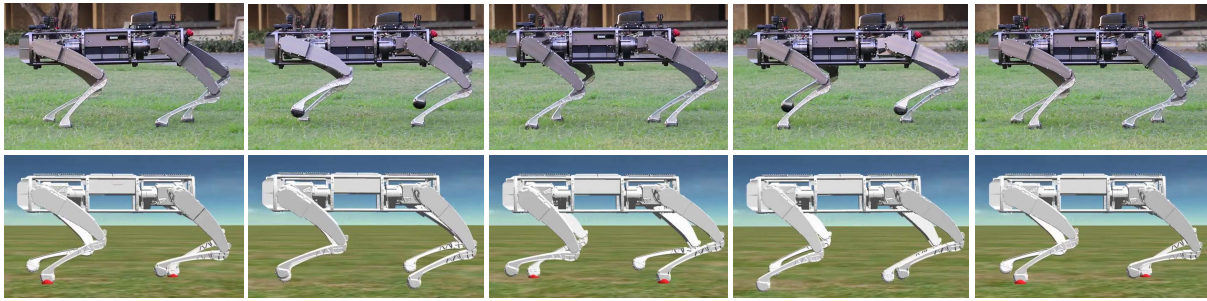


Fig. 5. *Top*: Snapshots showing a two full steps of the walking gait in an outdoor lawn. *Bottom*: Running gait in the RaiSim simulation environment.

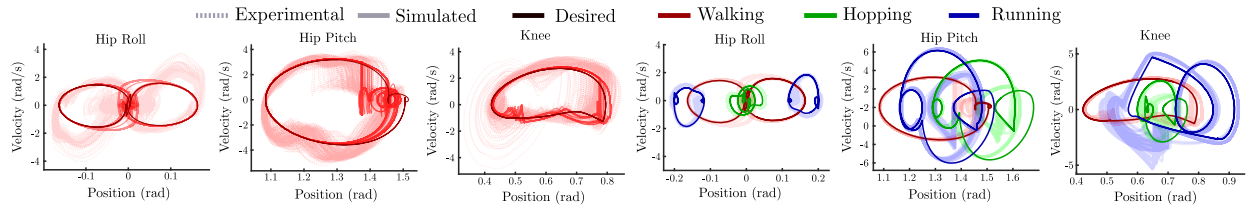


Fig. 6. *Left 3*: Experimental (dashed transparent) and simulated (solid transparent) phase portraits for walking plotted against the desired values (solid). *Right 3*: Simulated (transparent) versus desired (solid) phase portraits for walking (red), hopping (green), and running (blue) behaviors.

- [7] J. W. Grizzle, C. Chevallereau, R. W. Sinnet, and A. D. Ames, "Models, feedback control, and open problems of 3D bipedal robotic walking," *Automatica*, vol. 50, no. 8, pp. 1955 – 1988, 2014. [Online]. Available: <http://www.sciencedirect.com/science/article/pii/S0005109814001654>
- [8] A. Ames, K. Galloway, K. Sreenath, and J. Grizzle, "Rapidly exponentially stabilizing control lyapunov functions and hybrid zero dynamics," *Automatic Control, IEEE Transactions on*, vol. 59, no. 4, pp. 876–891, 2014.
- [9] K. Sreenath, H.-W. Park, I. Poulakakis, and J. W. Grizzle, "A compliant hybrid zero dynamics controller for stable, efficient and fast bipedal walking on mabel," *The International Journal of Robotics Research*, vol. 30, no. 9, pp. 1170–1193, 2011. [Online]. Available: <https://doi.org/10.1177/0278364910379882>
- [10] J. Reher, E. A. Cousineau, A. Hereid, C. M. Hubicki, and A. D. Ames, "Realizing dynamic and efficient bipedal locomotion on the humanoid robot DURUS," in *IEEE International Conference on Robotics and Automation (ICRA)*, 2016.
- [11] W. Ma, K. A. Hamed, and A. D. Ames, "First steps towards full model based motion planning and control of quadrupeds: A hybrid zero dynamics approach," in *2019 IEEE/RSJ International Conference on Intelligent Robots and Systems (IROS)*, 2019, pp. 5498–5503.
- [12] W.-L. Ma, N. Csomay-Shanklin, and A. D. Ames, "Coupled control systems: Periodic orbit generation with application to quadrupedal locomotion," *IEEE Control Systems Letters*, 2020.
- [13] W.-L. Ma and A. D. Ames, "From bipedal walking to quadrupedal locomotion: Full-body dynamics decomposition for rapid gait generation," in *IEEE International Conference on Robotics and Automation (ICRA)*, May 2020.
- [14] W.-L. Ma, N. Csomay-Shanklin, and A. D. Ames, "Quadrupedal robotic walking on sloped terrains via exact decomposition into coupled bipedal robots," in *IEEE International Conference on Intelligent Robots and Systems (IROS)*, Dec 2020.
- [15] R. Featherstone, *Rigid body dynamics algorithms*. Springer, 2014.
- [16] G. Antonelli, "Interconnected dynamic systems: An overview on distributed control," *IEEE Control Systems Magazine*, vol. 33, no. 1, pp. 76–88, 2013.
- [17] F. Dörfler and F. Bullo, "Synchronization in complex networks of phase oscillators: A survey," *Automatica*, vol. 50, no. 6, pp. 1539 – 1564, 2014. [Online]. Available: <http://www.sciencedirect.com/science/article/pii/S0005109814001423>
- [18] H. Fujisaka and T. Yamada, "Stability theory of synchronized motion in coupled-oscillator systems," *Progress of theoretical physics*, vol. 69, no. 1, pp. 32–47, 1983.
- [19] T. Hatanaka, N. Chopra, M. Fujita, and M. Spong, *Passivity-Based Control and Estimation in Networked Robotics*. Springer International Publishing, 2015.
- [20] Z. Jiang, I. Mareels, and Y. Wang, "A lyapunov formulation of nonlinear small gain theorem for interconnected systems," *IFAC Proceedings Volumes*, vol. 28, pp. 625–630, 1995.
- [21] M. Mesbahi and M. Egerstedt, *Graph theoretic methods in multiagent networks*. Princeton University Press, 2010, vol. 33.
- [22] W. Ren, R. W. Beard, and E. M. Atkins, "A survey of consensus problems in multi-agent coordination," in *Proceedings of the 2005, American Control Conference*, 2005. IEEE, 2005, pp. 1859–1864.
- [23] D. Mellinger, M. Shomin, N. Michael, and V. Kumar, *Cooperative Grasping and Transport Using Multiple Quadrotors*. Berlin, Heidelberg: Springer Berlin Heidelberg, 2013, pp. 545–558.
- [24] S.-J. Chung and J.-J. E. Slotine, "Cooperative robot control and concurrent synchronization of Lagrangian systems," *IEEE transactions on Robotics*, vol. 25, no. 3, pp. 686–700, 2009.
- [25] C. Sloth, "On the computation of lyapunov functions for interconnected systems," in *2016 IEEE Conference on Computer Aided Control System Design (CACSD)*, 2016, pp. 850–855.
- [26] K. A. Hamed, V. R. Kamidi, A. Pandala, W.-L. Ma, and A. D. Ames, "Distributed feedback controllers for stable cooperative locomotion of quadrupedal robots: A virtual constraint approach," *American Control Conference*, 2020.
- [27] R. M. Murray, Z. Li, S. S. Sastry, and S. S. Sastry, *A mathematical introduction to robotic manipulation*. CRC press, 1994.
- [28] A. Isidori, "The zero dynamics of a nonlinear system: From the origin to the latest progresses of a long successful story," in *Proceedings of the 30th Chinese Control Conference*, 2011, pp. 18–25.
- [29] S. Kolathaya, J. Reher, A. Hereid, and A. D. Ames, "Input to state stabilizing control Lyapunov functions for robust bipedal locomotion," in *2018 Annual American Control Conference (ACC)*, June 2018, pp. 2224–2230.
- [30] J. Hauser and Chung Choo Chung, "Converse lyapunov functions for exponentially stable periodic orbits," *Systems & Control Letters*, vol. 23, no. 1, pp. 27 – 34, 1994.
- [31] E. D. Sontag and Yuan Wang, "New characterizations of input-to-state stability," *IEEE Transactions on Automatic Control*, vol. 41, no. 9, pp. 1283–1294, 1996.
- [32] D. Angeli, "Input-to-state stability of pd-controlled robotic systems," *Automatica*, vol. 35, no. 7, pp. 1285 – 1290, 1999.
- [33] E. D. Sontag, *Control-Lyapunov functions*. London: Springer London, 1999, pp. 211–216.
- [34] W.-L. Ma. Simulation and experiments of quadrupedal walking with coupled clf-qps. Caltech. [Online]. Available: <https://youtu.be/D0LWc7VFxIM>
- [35] S. Nadubettu Yadukumar, "Input to state stabilizing control lyapunov functions for hybrid systems," Ph.D. dissertation, Georgia Institute of Technology, 2016.
- [36] S. Kolathaya and S. Veer, "Pd based robust quadratic programs for robotic systems," in *2019 IEEE/RSJ International Conference on Intelligent Robots and Systems (IROS)*, 2019, pp. 6834–6841.
- [37] J. Hwangbo, J. Lee, and M. Hutter, "Per-contact iteration method for solving contact dynamics," *IEEE Robotics and Automation Letters*, vol. 3, no. 2, pp. 895–902, 2018.